Radiation Physics and Chemistry 220 (2024) 111688

Contents lists available at ScienceDirect

Radiation Physics and Chemistry

journal homepage: www.elsevier.com/locate/radphyschem

# Development of lead-free metal carbides and ceramic decorated HDPE composites for low energy X-ray shielding applications

Kholoud S. Al-mugren [a], Layan Almalki [a], Razan Alshehri [a], Shahad Alamri [a], Mansour Almurayshid [b,*], Mohammed Alsuhybani [b], Rayan Alharbi [b], Mayeen Uddin Khandaker [c,d]

[a] Department of Physics, Science College, Princess Nourah Bint Abdulrahman University, Riyadh, Saudi Arabia
[b] Nuclear Technologies Institute, King Abdulaziz City for Science and Technology (KACST), Riyadh, Saudi Arabia
[c] Applied Physics and Radiation Technologies Group, CCDCU, School of Engineering and Technology, Sunway University, Bandar Sunway, 47500, Selangor, Malaysia
[d] Faculty of Graduate Studies, Daffodil International University, Daffodil Smart City, Birulia, Savar, Dhaka, 1216, Bangladesh

A R T I C L E I N F O

Handling Editor: Dr. Chris Chantler

A B S T R A C T

Materials with high atomic numbers are effective for shielding ionizing radiation. However, some, such as lead, are toxic, and their disposal causes environmental damage. Polymer composites are a good choice for radiation shielding because they are environmentally friendly, lightweight and non-toxic. This study investigated the possibility of using high-density polyethylenhe (HDPE) composites doped with three different materials comprising the carbide (such as tungsten carbide, and molybdenum carbide) and ceramic (silicon carbide) as a kilo-voltage radiation shield. The linear attenuation coefficients of the composites ranged from 0.21 to 2.82 $cm^{-1}$. The measured results are in good agreement with XCOM with an average error of 13.82%. Through meticulous empirical analysis, including the assessment of linear and mass attenuation coefficients, half-value layer (HVL), and mean free path (MFP), our findings suggest that HDPE composites doped with 15% MoC present the most promising configuration for low-energy X-ray shielding (30–50 keV). This work concludes that HDPE composites decorated with MoC and W could be used as an alternative and environment-friendly material for shielding of kilo-voltage X-rays in medical diagnostics and research environments.

## 1. Introduction

Nowadays, several ionizing radiations are widely used in various practical applications such as industrial inspection of device integrity via non-destructive techniques, scientific research, space exploration, nuclear engineering, medical imaging, and therapy (Wu et al., 2023). Among the various types of ionizing radiation, X-rays have demonstrated remarkable applications in the medical field, particularly in dentistry, mammography, and radiology. X-rays are electromagnetic radiation with wavelengths between 0.01 and 10 nm. They are classified into two forms, characteristics and bremsstrahlung. Characteristic X-rays are important because they can be used to produce quasi-monochromatic X-rays. Quasi-monochromatic X-rays have several advantages over polychromatic X-rays, including superior image quality and reduced patient dosage. This makes them ideal for use in applications such as coronary angiography, phase-contrast radiography, and mammography (Raza et al., 2013). On the other hand, Bremsstrahlung radiation is also widely employed in medicine, contributing significantly to the generation of photon spectra for diagnostic imaging and interventional radiology (Andreo et al., 2017).

Due to the extended use of radiation in various fields, the ALARA (As Low As Reasonably Achievable) principle is developed. and aims to minimize exposure to ionizing radiation by implementing proper shielding measures (Siegel et al., 2017). In Addition, the materials used in shielding design differ according to the type and energy of the radiation to be shielded (Almurayshid et al., 2021a; Can et al., 2021). Lead (Pb) is commonly employed as gamma and X-ray radiation shielding due to its high atomic number, high density, and high linear and mass attenuation coefficients, but it is also toxic and can have negative impacts on the environment. There is a need for sustainable radiation shielding materials that are non-toxic, flexible, lightweight, cost-effective and environmentally friendly (AbuAlRoos et al., 2019;

* Corresponding author.
*E-mail address:* malmurayshid@kacst.gov.sa (M. Almurayshid).

https://doi.org/10.1016/j.radphyschem.2024.111688
Received 24 November 2023; Received in revised form 4 March 2024; Accepted 10 March 2024
Available online 12 March 2024

Chen et al., 2023). In this regard, Polymer composites consist of a polymer matrix, such as polyethylene or polypropylene, reinforced with a filler material containing high atomic numbers, such as tungsten or molybdenum. High-density polyethylene (HDPE) is one of the most widely used plastics in the world due to its strength, moisture barrier, and solidity at room temperature. It is widely used and easily recycled, with no toxic emissions or poisonous chemical leaks (Mahmoud et al., 2018). Tungsten, with a density of 19.3 g cm-$^3$, exhibits good corrosion resistance, high heat/electrical conductivity, and a low expansion coefficient. For these reasons, tungsten can be employed as a substitute for Pb for gamma and X-ray shielding (Can et al., 2021). In addition, tungsten carbide (WC) is a widely used material for various applications due to its physical and mechanical features, including radiation shielding (Azman et al., 2023; Pak et al., 2020). The employment of tungsten carbide may provide a balance between low weight and high absorption (Giménez and Lopasso, 2018). Besides this, due to its mechanical strength, thermal conductivity, oxidation resistance, and radiation resistance, silicon carbide (SiC) has received a lot of attention from the scientific community (Yan et al., 2023). Moreover, silicone is the second most abundant element in the Earth's crust, making it a viable choice to use in shielding while also making it easier to mass produce (Kaur and Greger, 2019). Furthermore, molybdenum carbide (MoC) is an ideal material for radiation shielding in a range of adverse conditions. It has excellent electrical conductivity, and good thermal and chemical stability (Liu et al., 2020).

The polymer matrix imparts flexibility and processability to the material, while the inclusion of high atomic number fillers enhances its shielding effectiveness (AbuAlRoos et al., 2019; More et al., 2021; Pavlenko et al., 2019). However, there is still a gap in understanding how the properties of the polymer matrix and filler material impact the overall shielding effectiveness. For example, it is not yet clear how the properties of the polymer matrix and the filler affect the shielding effectiveness. This study aims to fill this knowledge gap and contribute to the development of advanced radiation shielding composites that not only offer effective protection but also meet the environmental and health safety standards required in medical settings. The outcomes of this study could lead to advancements in radiation protection technology, particularly in medical diagnostics and treatment procedures where minimizing radiation exposure is critical. The innovative aspect of our research lies in the detailed analysis of how different proportions of these fillers influence the shielding effectiveness against low-energy X-rays. Additionally, this study delves into the potential of these composites to provide safer, non-toxic, easy to be shaped, and environmentally friendly alternatives to conventional lead-based shielding materials. The overall objective of this study is to experimentally fabricate and investigate the potential use of low-weight shielding materials based on a mixture of HDPE polymer with proportions of silicon carbide (SiC), tungsten carbide (WC), and molybdenum carbide (MoC). We evaluate the X-ray shielding efficiency of the manfuctured polymer-based composites by analyzing various parameters, including the linear and mass attenuation coefficients (μ and $\mu_m$), half value layer (HVL), mean free path (MFP), and radiation protection efficacy (RPE). The findings of this study have the potential to lead to the development of new and improved radiation shielding materials that are non-toxic, lightweight, and environmentally friendly, thus addressing critical needs in various applications.

## 2. Theory on attenuation of radiation and relevant parameters

Photons interact with matter in various ways, which can be categorized based on the energy of the interacting photon, the type of target and the effect of the interaction on the photon (absorption or scattering). The removal of a photon from a gamma or X-ray beam based on the photoelectric effect, Compton scattering, or pair production is known as attenuation. The linear attenuation coefficient (μ), which can be stated as the likelihood that a photon would interact with matter per unit length, can be used to characterize this process (Jawad et al., 2019). Typically, when a greater reduction of radiation intensity is needed, the thickness of the interacting material is increased. This gives a longer path for X-rays to travel, giving a higher probability of absorption. The percentage of absorption for any material follows an exponentially rising curve where the percentage of intensity that is transmitted through a material gets exponentially less or shows an exponential decay curve as the thickness of the interacting material increases. This is empirically demonstrated as:

$$I(x) = I_o e^{-\mu x} \tag{1}$$

Where $I_o$ is the intensity of the incoming photon before interacting with the shielding material, $I$ is the intensity of the transmitted photon, i.e., after passing through the barrier, which is defined as the fractional drop of the interacting radiation (Halliwell et al., 2021; Thiele et al., 2021; Yasmin et al., 2018). The terms μ and $x$ in **Eq. (1)** represent the total linear attenuation coefficient ($cm^{-1}$) and material thickness respectively.

The mass attenuation coefficient ($\mu_m$) is another measure of a material's ability to absorb radiation. The $\mu_m$ is defined as the radiation attenuation performance per gram of the interacting material. The $\mu_m$ value is calculated by dividing the value of μ by the density (ρ) of the material, and it is independent of the material's physical state and density, as shown in **Eq. (2)** (Eren Belgin, 2022).

$$\mu_m = \mu / \rho \tag{2}$$

The most common quantitative measure for quantifying the ability of a particular radiation to penetrate the objects is the half-value layer (HVL). The term HVL refers to the thickness of a shield or any material where 50% of incoming energy has been attenuated. It is a substitute for measuring an X-ray spectrum's penetrability and is also known as beam quality. Like the attenuation coefficient, they depend on photon energy. HVL values offer helpful information regarding the radiation's ability to penetrate a certain substance (Almurayshid et al., 2021b; Alshareef et al., 2023). HVL is expressed by the following formula:

$$HVL = ln\ (2)\ / \mu \tag{3}$$

Additionally, the mean free path (MFP), measured in (cm), is the average separation between two consecutive interactions (Kumar, 2017). The formula used to measure it is as follows.

$$MFP = 1/\mu \tag{4}$$

where μ ($cm^{-1}$) represents the material's linear attenuation coefficient.

Radiation protection efficiency (RPE) could be used to evaluate the shielding capabilities of composite materials, depending on the linear attenuation coefficient (μ). The following relation can be used to obtain the RPE of any material (Naseer et al., 2021).

$$RPE = (1 - e^{\mu}) \times 100\ \ (\%) \tag{5}$$

## 3. Materials and methods

In this study, we chose HDPE, a thermoplastic polymer, which belongs to a class of polymers mainly derived from petrochemical feedstocks. compared to Low Density Polyethylene (LDPE), HDPE has outstanding properties such as tensile strength, moisture resistance, chemical resistance, and low cost, which makes it ideal for various industrial applications (Alkan et al., 2016; Kilic et al., 2017). Fig. 1 shows that various concentrations of SiC, MoC, and WC were used as fillers with the HDPE matrix in this study. HDPE's sample (density: 0.94 g/cm$^3$) was obtained from the Saudi Basic Industries Corporation (SABIC) (Riyadh, Saudi Arabia) and SiC (density: 3.21 g/cm$^3$), MoC (density: 8.90 g/cm$^3$) and WC (density: 15.63 g/cm$^3$)were provided by Thermo Fishers (Waltham, USA).

As shown in Table 1, sample A was 100% pure polyethylene, and

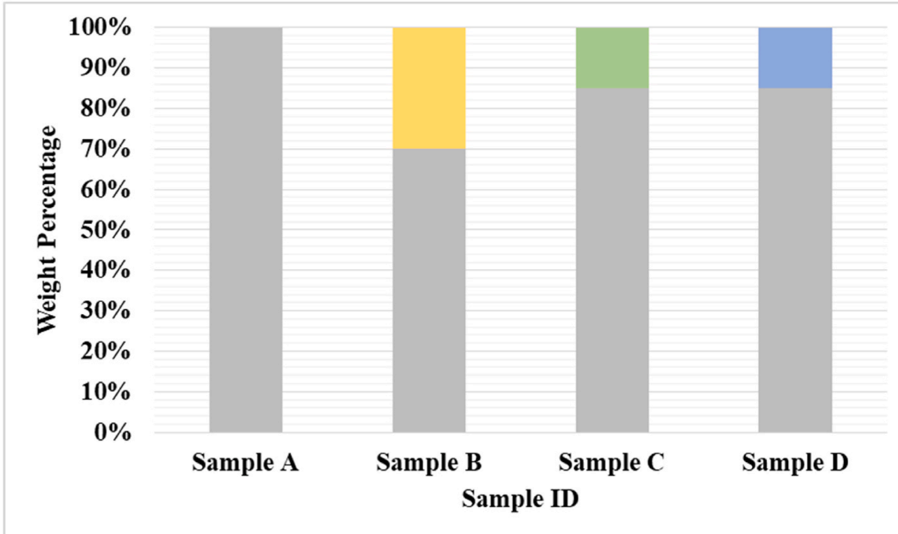


**Fig. 1.** Concentration of composite materials prepared in this study.

**Table 1**
Formulations of HDPE samples with different Additives.

| Sample ID | HDPE | Concentration of the additives |
|---|---|---|
| **A** | 100% | 0% |
| **B** | 70% | SiC (30%) |
| **C** | 85% | MoC (15%) |
| **D** | 85% | WC (15%) |

sample B contained 30% silicon carbide, which is not considered a metal and has a lower density, so its percentage in the composite was higher. Samples C and D only contained 15% of molybdenum carbide (MoC) and tungsten carbide (WC), respectively, which are considered heavy metals, making this concentration sufficient.

### *3.1. Preparation of HDPE-based composites*

All the experimental work including the sample preparation and irradiation were performed in the laboratories of the Nuclear Technologies Institute at King Abdulaziz City for Science and Technology (KACST). Fig. 2 depicts the manufacturing processes followed to produce the final shape of the sample.

#### *3.1.1. Material weighing process*

The volume of the chamber inside the mixer is approximately 400 ml, while the screw mixer occupies 30% of the said volume, meaning that the 70% left is to be filled with the polymer composites, so the remaining 280 ml must be filled to get the best sample. Therefore, we measure the weight of the prepared material according to the following equation:

$$W = \rho V \tag{6}$$

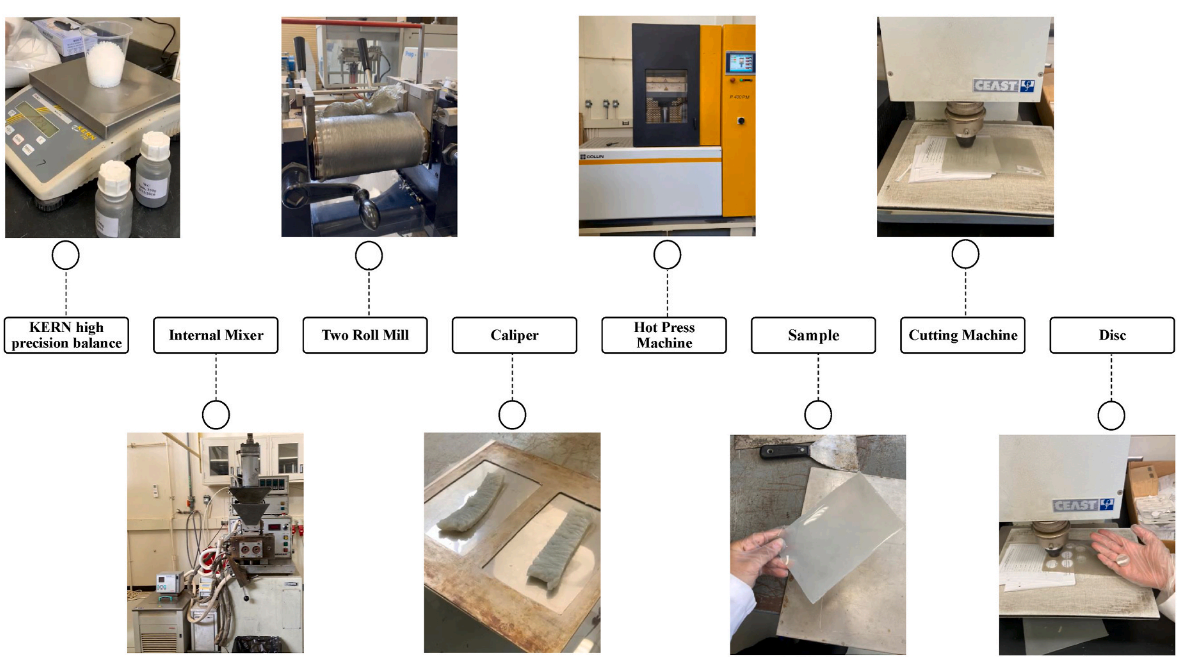


**Fig. 2.** Steps of fabrication four different samples into discs.

Where, $W$ is the weight of the material, $\rho$ is its density, and $V$ is the volume.

Since the prepared samples are composite, therefore first we need to obtain the total density of each sample. It was calculated using the following method. As an example for sample C, we add the density of tungsten carbide multiplied by its percentage (15%) with the density of the HDPE multiplied by its percentage (85%). Then we multiply the total density by the volume of the chamber to obtain the weight of the respective sample. For simplicity, the mathematical formulations are given as follows,

$$\rho_{wc} = 15.63 \times 0.15 = 2.3445 \text{ g/cm}^2$$

$$\rho_{HDPE} = 0.93 \times 0.85 = 0.7905 \text{ g/cm}^2$$

$$\rho_t = 2.3445 + 0.7905 = 3.135 \text{ g/cm}^2$$

$$W = \rho_t V = 3.135 \times 280 = 877.8 \text{ g}$$

Following the aforementioned process, the density and weight of the other samples are obtained in the same manner.

#### *3.1.2. Composites mixing*

After determining the weight of each sample, the HDPE composite samples were heated for a period of 5–6 min at a temperature of 178 °C in the chamber of the internal mixer to dissolve them and to obtain the best homogeneity. The composite was then transferred to the two roll mills and run for 5 min (set at 195 °C and 10 rpm) to provide homogeneous mixing properties.

#### *3.1.3. Composites formation*

After that, we put the composite in a metal frame to press it in a hot press machine (Collin P 400 p.m., Ebersberg, Germany), and to determine the weight of the exact amount to be filled in, we obtained the volume of the rectangle and multiply it by the density of each composite. For instance, sample C (HDPE-WC), its weight must be equal to 124.146 g.

#### *3.1.4. Composites cutting*

After the composite came out from the hot press machine, it was allowed to cool down at room temperature for 2 h, then we cut it into small discs with a diameter of 5 cm by using the cutting machine (Ceast, Pianezza, Italy).

## 4. Experimental setup

An X-ray unit situated at the radiation calibration laboratory of KACST was used to determine the radiation protection efficiency of the studied composite samples. A reference calibration quality presented in Table 2, was used to calibrate the diagnostic radiology devices, and it was employed to calculate μ given in **Eq. (1)**. An ionization chamber was set at 100 cm away from the x-ray focal point as shown in Fig. 3. The sample was positioned at 50 cm away from the X-ray source. The experiment began by exposing the detector to X-rays without using the shield disk, and the values were recorded as $I_o$ for seven different energies of 30, 33, 36.2, 37.7, 39.6, 44.3, and 50 keV, and a current of 10 mA. Then, pure HDPE shield discs were placed in the way of the X-ray to obtain the value of attenuated intensity $I$ and repeated the steps for all HDPE-based composite shield discs. The shielding effectiveness of HDPE composites manufactured as discs was investigated for 1 cm thicknesses for each composite.

An ionization chamber and electrometer were managed by the Pico Ampere Meter W2006 (PAMW2006) software and were used in this study. The entire experiment was set up in the middle of the room, 158 cm above the floor, to prevent scuffing on the walls and flooring. An average of three readings was calculated for each energy and sample. By examining the μ, the shielding efficacy could be emphasized through other shielding parameters such as $\mu_m$, HVL, MFP and RPE using Equations 2, 3, 4 and 5, respectively. At the end of the experimental work, and after determining the μ for each sample empirically, we compared these outputs mathematically using the Xcom software, to calculate the percentage of error.

**Table 2**
The reference calibration qualities used for irradiation of the samples showing the applied voltage, the filtration and effective energy, $\mathbf{E}_{eff}$.

| Quality | Tube voltage, kVp | Total filtration, mm AI | Effective Energy ($\mathbf{E}_{eff}$), keV |
|---|---|---|---|
| RQR 4 | 60 | 2.68 | 30.0 |
| RQR 5 | 70 | 2.83 | 33.0 |
| RQR 6 | 80 | 2.99 | 36.2 |
| RQR 7 | 90 | 3.18 | 37.7 |
| RQR 8 | 100 | 3.36 | 39.6 |
| RQR 9 | 120 | 3.73 | 44.3 |
| RQR 10 | 150 | 4.38 | 50.0 |

## 5. Results and discussion

This study used μ to calculate the radiation shielding efficiency of HDPE polymer composites in attenuating the X-ray energy range of 30–50 keV. Shielding materials based on the HDPE polymer were suggested and created, and they were blended with various concentrations (15% and 30%) of three different materials comprising the carbide (such as tungsten carbide, and molybdenum carbide) and ceramic (silicon carbide). The proposed shielding materials were produced and cut into disks, which were found to be lighter than Pb.

### *5.1. Linear attenuation coefficient, μ*

Fig. 4 shows that the μ of HDPE and HDPE-SiC samples are close and very low with energy, and this means that SiC ceramic is not as effective shield as samples C (HDPE-MoC) and D (HDPE-WC). Sample C containing MoC shows the strongest shield at 30 keV energy, and close to sample D. Fig. 4 shows that as X-ray energies increased, the value of μ is decreased. The overall results strongly imply that energy plays a role in the contrast of μ with X-rays, which is caused by the numerous photon-material interactions.

### *5.2. Mass Attenuation coefficient ($\mu_m$)*

The HDPE samples containing metallic carbides have the largest mass attenuation coefficient ($\mu_m$) across all photon energies when compared to ceramic (SiC) decorated HDPE samples (see Table 4). This might be due to the presence of components with large atomic numbers and their high density. The HDPE- MoC and HDPE-WC have much better X-ray shielding capabilities than the pure HDPE. The differences also become noticeable at low energies, particularly at 30 keV. This demonstrates how essential it is to include heavy metals in the HDPE polymer to provide radiation protection at these low energies, which are commonly used in diagnostic procedures in radiation research centers and medical physics centers. The experimental values of the mass attenuation factor $\mu_m$ were then compared with the theoretical values (XCOM database), which were compiled by NIST and plotted against energy changes. The observed phenomenon in Fig. 5, where HDPE + MoC demonstrates greater mass attenuation than HDPE + WC, can be attributed to the complex interplay of material properties and X-ray interaction mechanisms. Despite WC's higher density and atomic number, MoC's specific electronic structure may favor enhanced X-ray attenuation at the studied energies. This suggests that factors beyond simple density and atomic number, such as the material's microstructure and photon absorption behavior, critically influence shielding effectiveness. This unexpected result underscores the importance of

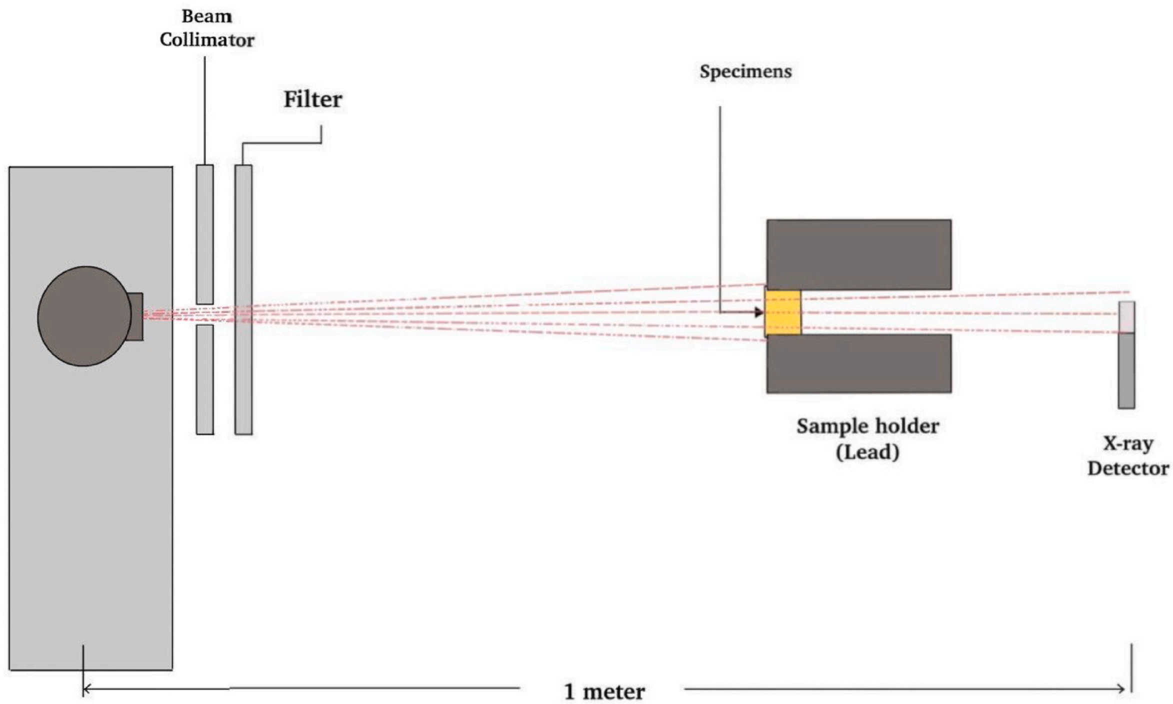


**Fig. 3.** Schematic illustration of the setup used for the measurement of the attenuation of X-ray. A collimator, with a 5 cm diameter, was used and the samples positioned in a holder 50 cm away from the X-ray source. The ionization chamber was put 15 cm from the sample holder.

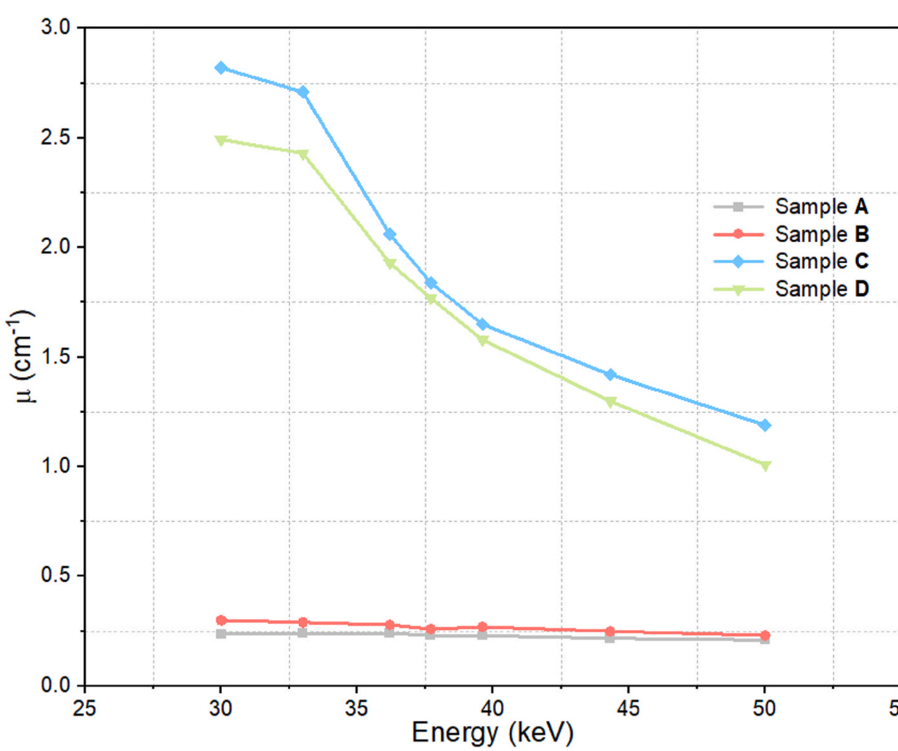


**Fig. 4.** Linear attenuation coefficient ($cm^{-1}$) against the X-ray energy (keV).

comprehensive material analysis in developing efficient radiation shielding. The percentage error of the mass attenuation was calculated according to Eq. (7) for all samples at each specific energy through repeated measurements, and then the standard deviation was obtained. The standard deviation was very small, so error bars were excluded.

$$\textit{Percent Error} = \frac{|\textit{measured} - \textit{real}|}{\textit{real}} \times \mathbf{100}\ (\%) \tag{7}$$

The average for all samples amounted to 13.82%, where the error percentages for each sample were varied as A-3.32%, B-11.93%, C-21.12%, and D-18.82%.

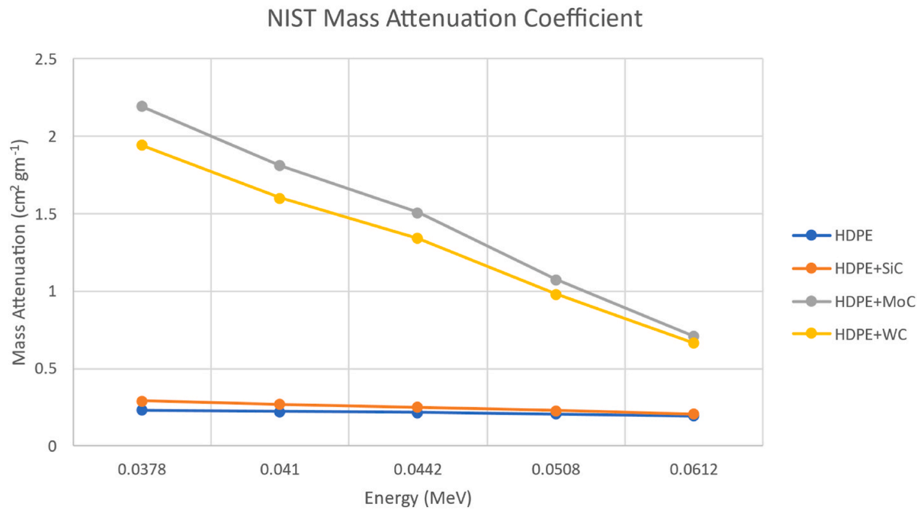


**Fig. 5.** Mass attenuation coefficient against the energy.

### 5.3. *Half value layer (HVL)*

The HVL is expressed as a distance, and it is a photon energy-dependent parameter. It is the thickness of a material at which half of the incident energy is attenuated. The HVL of a material becomes larger as the penetrating energy of a photon stream increases. As shown in Fig. 6, the HDPE-MoC and HDPE-WC have absorbed more energy, so the HVL was very small compared to the HDPE, where the HVL was very large, which means that the penetration is high, meaning a large proportion of the X-rays was not absorbed.

### 5.4. *Mean free path (MFP)*

The average distance between two subsequent interactions of photons with the materials is measured by the MFP. Fig. 7 includes an estimation of the attenuation capabilities of HDPE-based composites across the energy range from 30 to 50 keV. According to **Eq. (4)**, this parameter is inversely proportional to the linear attenuation coefficient. The MFP values could confirm the efficiency of the HDPE composites under this study for X-ray shielding applications. The overall tendency for the MFP was found to rise rapidly with increasing energy. Fig. 7 shows that the MFP is lower when photon energy is low and higher when photon energy increases. It is clear that the excess heavy metal content in the polymer composite has a substantial impact on the shielding performance of this HDPE polymer. As a result, MFP values decrease as sample density increases. Pure HDPE composite has the highest MFP, while (HDPE-MoC) and (HDPE-WC) composites have the lowest MFP. The highest densities and masses give the best X-ray shielding capabilities among our studied composites. We determined that the HDPE-based composites which contain heavy metal carbides like WC and

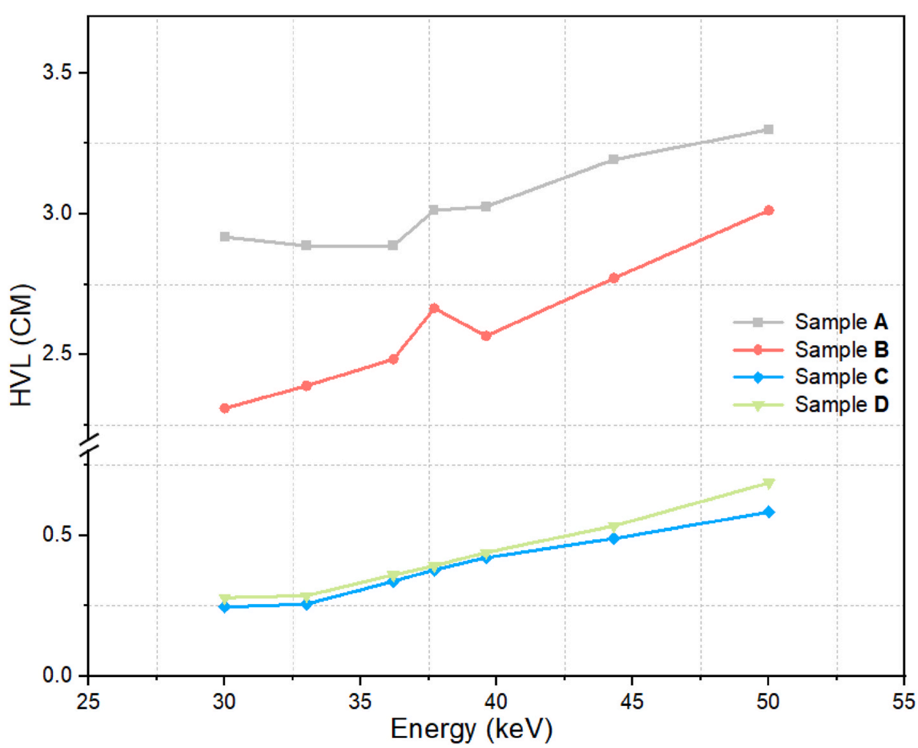


**Fig. 6.** Half Value-Layer of the studied samples at various energy values.

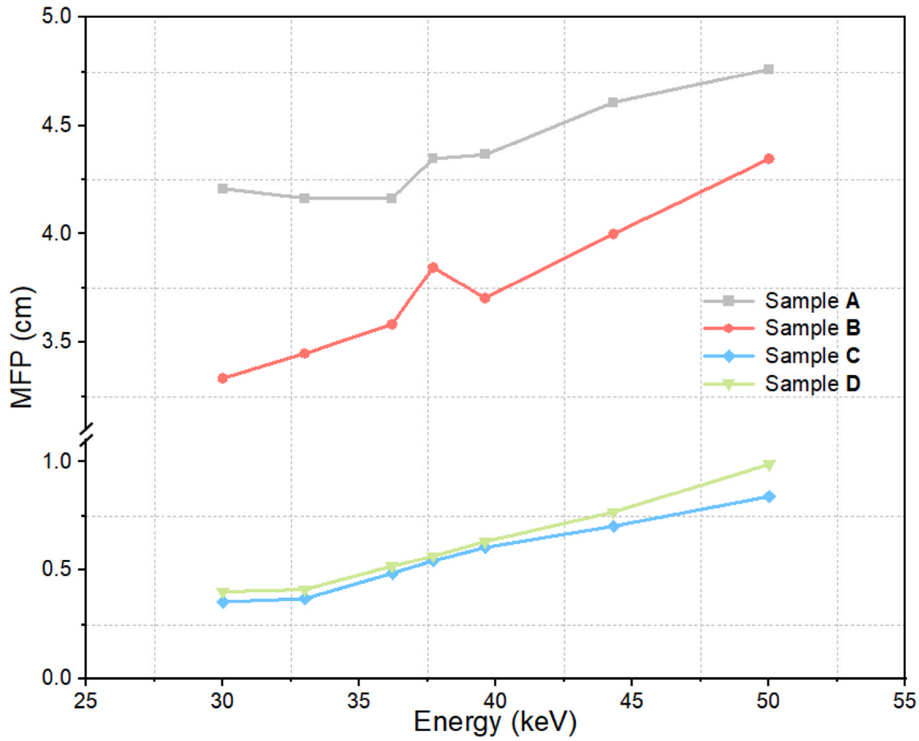


**Fig. 7.** Mean Free Path of the studied samples at various X-ray energy values.

MoC were more effective in shielding than other elements like SiC.

### 5.5. Radiation protection efficiency (RPE)

The RPE of all HDPE-based composites at various energies from 30 to 50 keV were estimated using Eq. (5) and the results are presented in Table 3. At lower energies, it was found that samples D containg MoC has the highest percentage reaching 94.04%. Similarly, at the higher energies, the RPE is reached to 75.83% at 44.3 keV energy. This shows that the range of low photon energies has a higher RPE than the range of high photon energies.

## 6. Conclusion

This study introduces innovative high-density polyethylene (HDPE) composites with metal carbides (MoC,WC) and ceramic (SiC) as effective kilo-voltage X-ray shielding materials. Our research highlights that these composites significantly enhance X-ray attenuation, particularly in low-energy ranges, presenting a non-toxic and lightweight alternative to traditional shielding materials like lead. The HDPE + MoC composite, in particular, demonstrates higher shielding capabilities at 50 keV than other manufactured samples, suggesting its potential for safer medical diagnostic environment by using a thicker shield or increasing the percentage of the concentration of heavy metals. Future research should focus on optimizing composite formulations for broader radiation types, and evaluating long-term durability. By advancing these materials, we aim to improve radiation safety in healthcare and beyond, reducing reliance on hazardous substances and promoting environmental sustainability.

**Table 3**
Mass attenuation coefficient of the HDPE composites samples.

| Photon Energy (keV) | Mass Attenuation Coefficient $\mu_m$ ($cm^2gm^{-1}$) | | | | | | | |
|---|---|---|---|---|---|---|---|---|
| | Measured | | | | Calculated | | | |
| | A | B | C | D | A | B | C | D |
| 30 | 0.24 | 0.28 | 2.52 | 2.26 | 0.27 | 0.35 | 3.88 | 3.88 |
| 33 | 0.24 | 0.27 | 2.42 | 2.21 | 0.25 | 0.31 | 2.96 | 3.20 |
| 36.2 | 0.24 | 0.26 | 1.84 | 1.75 | 0.24 | 0.28 | 2.32 | 2.70 |
| 37.7 | 0.23 | 0.24 | 1.64 | 1.61 | 0.23 | 0.27 | 2.14 | 2.16 |
| 39.6 | 0.23 | 0.25 | 1.47 | 1.43 | 0.23 | 0.25 | 1.90 | 1.96 |
| 44.3 | 0.22 | 0.23 | 1.27 | 1.18 | 0.22 | 0.23 | 1.47 | 1.36 |
| 50 | 0.21 | 0.21 | 1.06 | 0.92 | 0.21 | 0.21 | 1.07 | 1.01 |

**Table 4**
Radiation protection efficiency of the HDPE composites samples.

| Photon Energy | Radiation Protection Efficiency (%) | | | |
|---|---|---|---|---|
| (keV) | A | B | C | D |
| **30** | 21.14 | 25.92 | 94.04 | 91.73 |
| **33** | 21.34 | 25.17 | 93.35 | 91.20 |
| **36.2** | 21.34 | 24.35 | 87.25 | 85.49 |
| **37.7** | 20.55 | 22.89 | 84.12 | 82.97 |
| **39.6** | 20.47 | 23.66 | 80.80 | 79.40 |
| **44.3** | 19.51 | 22.12 | 75.83 | 72.75 |
| **50** | 18.94 | 20.55 | 69.58 | 63.58 |

## Recommendation

We strongly recommend the development of the polymer composite doped with MoC as a low-energy radiation shield as it reaches a 70% RPE at 50 keV as well as the composite doped with WC. We do not recommend SiC ceramic doped composite which only had 20% RPE at 50 keV.

## CRediT authorship contribution statement

**Kholoud S. Al-mugren:** Writing – review & editing, Writing – original draft, Visualization, Validation, Supervision, Funding acquisition, Data curation, Conceptualization. **Layan Almalki:** Writing – review & editing, Writing – original draft, Validation, Methodology, Formal analysis, Data curation. **Razan Alshehri:** Writing – review & editing, Writing – original draft, Validation, Project administration, Methodology, Formal analysis, Data curation. **Shahad Alamri:** Writing – review & editing, Writing – original draft, Validation, Methodology, Formal analysis, Data curation. **Mansour Almurayshid:** Writing – review & editing, Writing – original draft, Methodology, Data curation, Conceptualization. **Mohammed Alsuhybani:** Conceptualization, Methodology. **Rayan Alharbi:** Methodology. **Mayeen Uddin Khandaker:** Writing – review & editing, Writing – original draft.

## Declaration of competing interest

The authors declare that they have no known competing financial interests or personal relationships that could have appeared to influence the work reported in this paper.

## Data availability

No data was used for the research described in the article.

## Acknowledgments

The authors express their sincere thanks to Princess Nourah bint Abdulrahman University, Riyadh, Saudi Arabia, for generously funding this research under the Princess Nourah bint Abdulrahman University Researchers Supporting Project (PNURSP2024R10). Our gratitude also extends to the King Abdulaziz City for Science and Technology for providing the vital laboratory resources and equipment necessary for the completion of this study.

## References

AbuAlRoos, N.J., Baharul Amin, N.A., Zainon, R., 2019. Conventional and new lead-free radiation shielding materials for radiation protection in nuclear medicine: a review. Radiat. Phys. Chem. 165, 108439 https://doi.org/10.1016/J.RADPHYSCHEM.2019.108439.

Alkan, Ü., Kiliç, M., Karabul, Y., Yamak, H.B., Okutan, M., Içelli, O., 2016. Electrical and mechanical properties of LDPE/PANI composites. J. Nanoelectron. Optoelectron. 11 (3), 343–348. https://doi.org/10.1166/JNO.2016.1889.

Almurayshid, M., Alsagabi, S., Alssalim, Y., Alotaibi, Z., Almsalam, R., 2021a. Feasibility of polymer-based composite materials as radiation shield. Radiat. Phys. Chem. 183, 109425 https://doi.org/10.1016/j.radphyschem.2021.109425.

Almurayshid, M., Alssalim, Y., Aksouh, F., Almsalam, R., Alqahtani, M., Sayyed, M.I., Almasoud, F., 2021b. Development of new lead-free composite materials as potential radiation shields. Materials 2021 14 (17), 4957. https://doi.org/10.3390/MA14174957.

Alshareef, R., Marashdeh, M.W., Almurayshid, M., Alsuhybani, M., 2023. Study of radiation attenuation properties of HDPE/ZnO at energies between 47.5 and 266 keV. Prog. Nucl. Energy 165, 104909. https://doi.org/10.1016/J.PNUCENE.2023.104909.

Andreo, P., Burns, D., Nahum, A., Seuntjens, J., Attix, F., 2017. Fundamentals of Ionizing Radiation Dosimetry, first ed. Wiley-Vch.

Azman, M.N., Abualroos, N.J., Yaacob, K.A., Zainon, R., 2023. Feasibility of nanomaterial tungsten carbide as lead-free nanomaterial-based radiation shielding. Radiat. Phys. Chem. 202, 110492 https://doi.org/10.1016/J.RADPHYSCHEM.2022.110492.

Can, Ö., Eren Belgin, E., Aycik, G.A., 2021. Effect of different tungsten compound reinforcements on the electromagnetic radiation shielding properties of neopentyl glycol polyester. Nucl. Eng. Technol. 53 (5), 1642–1651. https://doi.org/10.1016/J.NET.2020.11.006.

Chen, Z., Li, X., Lu, L., Yuan, B., Wang, L., Li, Z., Li, H., 2023. Non-toxic and flexible radiation-shielding composites based on natural rubber containing elemental W fillers for efficient shielding against X/γ-rays. Processes 2023 11 (3), 674. https://doi.org/10.3390/PR11030674.

Eren Belgin, E., 2022. Comparison of gamma spectrometric method and XCOM method in calculating mass attenuation coefficients of reinforced polymeric composite materials. Radiat. Phys. Chem. 193, 109960 https://doi.org/10.1016/J.RADPHYSCHEM.2022.109960.

Giménez, M.A.N., Lopasso, E.M., 2018. Tungsten carbide compact primary shielding for small medium reactor. Ann. Nucl. Energy 116, 210–223.

Halliwell, E., Couch, C., Begum, R., Li, W., Maqbool, M., 2021. Increase in linear attenuation coefficient by changing crystal structure of materials for radiation shielding and biomedical devices safety. Colloids Surf. A Physicochem. Eng. Asp. 622, 126646 https://doi.org/10.1016/J.COLSURFA.2021.126646.

Jawad, A.A., Demirkol, N., Gunoğlu, K., Akkurt, I., 2019. Radiation shielding properties of some ceramic wasted samples. Int. J. Environ. Sci. Technol. 16 (9), 5039–5042. https://doi.org/10.1007/S13762-019-02240-7/METRICS.

Kaur, H., Greger, M., 2019. A review on Si uptake and transport system. Plants 2019 8 (4), 81. https://doi.org/10.3390/PLANTS8040081.

Kilic, M., Karabul, Y., Alkan, U., Yagci, O., Okutan, M., Icelli, O., 2017. Gamma-ray irradiation effect on mechanical and dielectric properties of volcanic basalt mineral reinforced low density polyethylene films. Physicochem. Probl. Miner. Process. 53 (1), 578–590. https://doi.org/10.5277/PPMP170145.

Kumar, A., 2017. Gamma ray shielding properties of PbO-Li2O-B2O3 glasses. Radiat. Phys. Chem. 136, 50–53. https://doi.org/10.1016/J.RADPHYSCHEM.2017.03.023.

Liu, X., Xu, H., Xie, F., Fasel, C., Yin, X., Riedel, R., 2020. Highly flexible and ultrathin Mo2C film via in-situ growth on graphene oxide for electromagnetic shielding application. Carbon 163, 254–264. https://doi.org/10.1016/J.CARBON.2020.03.003.

Mahmoud, M.E., El-Khatib, A.M., Badawi, M.S., Rashad, A.R., El-Sharkawy, R.M., Thabet, A.A., 2018. Recycled high-density polyethylene plastics added with lead oxide nanoparticles as sustainable radiation shielding materials. J. Clean. Prod. 176, 276–287. https://doi.org/10.1016/J.JCLEPRO.2017.12.100.

More, C.V., Alsayed, Z., Badawi, M.S., Thabet, A.A., Pawar, P.P., 2021. Polymeric composite materials for radiation shielding: a review. Environmental Chemistry Letters 2021 19 (3), 2057–2090. https://doi.org/10.1007/S10311-021-01189-9.

Naseer, K.A., Marimuthu, K., Mahmoud, K.A., Sayyed, M.I., 2021. Impact of Bi2O3 modifier concentration on barium–zincborate glasses: physical, structural, elastic, and radiation-shielding properties. The European Physical Journal Plus 2021 136 (1), 1–23. https://doi.org/10.1140/EPJP/S13360-020-01056-6.

Pak, A.Y., Shanenkov, I.I., Mamontov, G.Y., Kokorina, A.I., 2020. Vacuumless synthesis of tungsten carbide in a self-shielding atmospheric plasma of DC arc discharge. Int. J. Refract. Metals Hard Mater. 93, 105343 https://doi.org/10.1016/J.IJRMHM.2020.105343.

Pavlenko, V.I., Cherkashina, N.I., Yastrebinsky, R.N., 2019. Synthesis and radiation shielding properties of polyimide/Bi 2 O 3 composites. Heliyon 5 (5), e01703. https://doi.org/10.1016/j.heliyon.2019.e01703.

Raza, H.S., Kim, H.J., Ha, J.M., Cho, S.O., 2013. Behavior of characteristic X-rays from a partial-transmission-type X-ray target. Appl. Radiat. Isot. 80, 67–72. https://doi.org/10.1016/j.apradiso.2013.06.009.

Siegel, J.A., McCollough, C.H., Orton, C.G., 2017. Advocating for use of the ALARA principle in the context of medical imaging fails to recognize that the risk is hypothetical and so serves to reinforce patients' fears of radiation. Med. Phys. 44 (1), 3–6. https://doi.org/10.1002/MP.12012.

Thiele, K.T., Alexander, R.W., Maqbool, M., 2021. Characterization of 83Bi209, 74W184, 48Cd112, 30Zn65, 28Ni59 and 26Fe56 using Modified Klein-Nishina formula, for radiation shielding and dosimetry. Radiat. Phys. Chem. 179, 109264 https://doi.org/10.1016/J.RADPHYSCHEM.2020.109264.

Wu, J., Hu, J., Wang, K., Zhai, Y., Wang, Z., Feng, Y., Fan, H., Wang, K., Duan, Y., 2023. Flexible stretchable low-energy X-ray (30–80 keV) radiation shielding material: low-melting-point Ga1In1Sn7Bi1 alloy/thermoplastic polyurethane composite. Appl. Radiat. Isot. 192, 110603 https://doi.org/10.1016/j.apradiso.2022.110603.

Yan, Z., Liu, R., Liu, B., Shao, Y., Liu, M., 2023. Molecular dynamics simulation studies of properties, preparation, and performance of silicon carbide materials: a review. Energies 16 (3), 1176.

Yasmin, S., Rozaila, Z.S., Khandaker, M.U., Barua, B.S., Chowdhury, F.U.Z., Rashid, M.A., Bradley, D.A., 2018. The radiation shielding offered by the commercial glass installed in Bangladeshi dwellings. Radiat. Eff. Defect Solid 173 (7–8), 657–672. https://doi.org/10.1080/10420150.2018.1493481.